**RESEARCH ARTICLE**

Methods in Ecology and Evolution | BRITISH ECOLOGICAL SOCIETY

# SuessR: Regional corrections for the effects of anthropogenic $CO_2$ on $\delta^{13}C$ data from marine organisms

Casey T. Clark[1,2] 🅐　|　Mattias R. Cape[3] 🅐　|　Mark D. Shapley[4] 🅐　|　Franz J. Mueter[5] 🅐　|
Bruce P. Finney[6] 🅐　|　Nicole Misarti[2] 🅐

[1]Cooperative Institute for Climate, Ocean, and Ecosystem Studies, University of Washington, Seattle, WA, USA; [2]Water and Environmental Research Center, University of Alaska Fairbanks, Fairbanks, AK, USA; [3]School of Oceanography, University of Washington, Seattle, WA, USA; [4]CDSCO/National Lacustrine Core Facility, University of Minnesota, Minneapolis, MN, USA; [5]College of Fisheries and Ocean Sciences, University of Alaska Fairbanks, Juneau, AK, USA and [6]Departments of Biological Sciences and Geosciences, Idaho State University, Pocatello, ID, USA

**Correspondence**
Casey T. Clark
Email:casey.t.clark@gmail.com

**Abstract**

1. Anthropogenic $CO_2$ emissions associated with fossil fuel combustion have caused declines in baseline oceanic $\delta^{13}C$ values. This phenomenon, called the Suess effect, can confound comparisons of marine $\delta^{13}C$ data from different years. The Suess effect can be corrected for mathematically; however, a variety of disparate techniques are currently used, often resulting in corrections that differ substantially. SuessR is a free, user-friendly tool that allows researchers to calculate and apply regional Suess corrections to $\delta^{13}C$ data from marine systems using a unified approach.

2. SuessR updates existing methods for calculating region-specific Suess corrections for samples collected from 1850 to 2020. It also estimates changes in phytoplankton $^{13}C$ fractionation associated with increasing water temperature and aqueous $CO_2$ concentrations, referred to here as the Laws effect. SuessR version 0.1.3 contains four built-in regions, including three in the subpolar North Pacific (Bering Sea, Aleutian Islands and Gulf of Alaska) and one North Atlantic region (Subpolar North Atlantic). Users can also supply environmental data for regions not currently built into SuessR to generate their own custom corrections.

3. In 2020, net corrections (Suess + Laws corrections) were as follows—Bering Sea: 1.29‰; Aleutian Islands: 1.30‰, Gulf of Alaska: 1.30‰; and Subpolar North Atlantic: 1.31‰ (compared to a global atmospheric $CO_2$ change of ~2.43‰ across the same period). For samples collected in 2020, the net correction exceeds instrumental error ($\pm0.2$‰) when making comparisons across only eight years (i.e. 2013–2020). The magnitude of the Suess effect calculated by SuessR aligns with published estimates, whereas the Laws effect is smaller than previously calculated, resulting from updated estimates of average community cell sizes, growth

rates and permeability of phytoplankton plasmalemmas (the plasma membrane which bounds the cell) to $CO_2$.

4. The increasing magnitude of the Suess effect means this phenomenon is no longer only of concern to historical ecologists, but now affects contemporary ecological studies using $\delta^{13}C$ data. This highlights the importance of a unified approach for generating Suess corrections. The SuessR package provides a customizable tool that is simple to use and will improve the interpretability and comparability of future stable isotopic studies of marine ecology.

## 1 | INTRODUCTION

Anthropogenic emissions of carbon dioxide, primarily through combustion of fossil fuels, have altered the baseline $\delta^{13}C$ values of the planet's atmosphere and oceans since the Industrial Revolution (Keeling, 1979). This $\delta^{13}C$ decline is commonly referred to as the Suess effect, and has been increasing in magnitude exponentially, in tandem with the exponential increase in $^{13}C$-depleted $CO_2$ emissions (Bacastow et al., 1996). The shifting $\delta^{13}C$ baseline is incorporated into biological systems by way of photosynthetic organisms, which fix ambient $CO_2$. These effects propagate throughout food webs, as the stable carbon isotopes of primary producers are incorporated into the tissues of consumers. For ecologists seeking to examine changes in $\delta^{13}C$ values over time to understand animal migratory movements, food web structure and trophic interactions, as well as animal and plant physiology, the Suess effect has the potential to confound analyses (Misarti et al., 2009).

In addition to the shifts in $\delta^{13}C$ that characterize the Suess effect, increasing atmospheric $CO_2$ concentrations affect plant physiology in ways that may impact stable carbon isotope fractionation during photosynthesis (Keeling et al., 2017). In marine and aquatic systems, $^{13}C$ fractionation by phytoplankton changes in relation to water temperature and aqueous $CO_2$ concentrations (Laws et al., 2002). Thus, warming of the global oceans observed in recent decades, as well as substantial increases in atmospheric and aqueous $CO_2$ concentrations during this same period, has also altered baseline $\delta^{13}C$ values in marine ecosystems. The impacts of water temperature (via community composition and growth rates) and aqueous $CO_2$ concentrations on stable carbon isotope fractionation by phytoplankton were described mathematically by Laws et al. (2002), and are hereafter referred to as the Laws effect.

Efforts have been made to quantify and mathematically correct for the Suess and Laws effects, primarily by historical ecologists, palaeoecologists and archaeologists comparing $\delta^{13}C$ values across broad timeframes. These researchers typically correct historic and modern values back to preindustrial times (i.e. the year 1850, the onset of the Industrial era and the beginning of exponential increases in anthropogenic $CO_2$ emissions into the atmosphere and oceans; Ruddiman, 2013). However, as the burning of fossil fuels has continued to produce exponentially increasing releases of anthropogenic $CO_2$ (Bacastow et al., 1996), the year-to-year changes in the magnitude of the Suess effect (and to a lesser extent, the Laws effect) have increased substantially. As of 2020, the summed magnitude of the Suess and Laws corrections for $\delta^{13}C$ values from the Bering Sea, calculated using the methods described in this paper, exceeds the typically reported value for instrumental precision for isotope ratio mass spectrometers ($\pm 0.2‰$) when comparing samples across just 8 years (i.e. comparing samples from 2020 to samples from 2013; Figure 1). Thus, the Suess and Laws effects introduce detectable error in comparisons of modern stable carbon isotope data collected over less than a decade. This suggests that corrections for the Suess and Laws effects are no longer only the concern of historical ecologists, palaeoecologists and archaeologists, and that these corrections should be incorporated into contemporary ecological studies comparing isotope values over spans of 8 years or more. Although calculation of mathematical Suess corrections has become relatively commonplace, the methods used vary widely and can produce substantially different results (Figure 1), highlighting the need for a unified approach to calculate Suess and Laws corrections for $\delta^{13}C$ data.

The SuessR package is a tool for calculating and applying mathematical corrections for the Suess and Laws effects. These corrections are region-specific, accounting for the complex spatial variability in seawater circulation, surface residence time, water temperature and biological production that impact $CO_2$ uptake by the oceans (Eide et al., 2017), as compared with the relatively homogeneous and well-mixed global atmosphere. The purpose of this R package is to provide a simple and effective tool that allows ecologists to apply these corrections to $\delta^{13}C$ data from marine systems using a single, unified methodology. Additionally, users will be able to supply their own region-specific parameters to the Suess and Laws corrections, and are encouraged to submit these data for incorporation into the
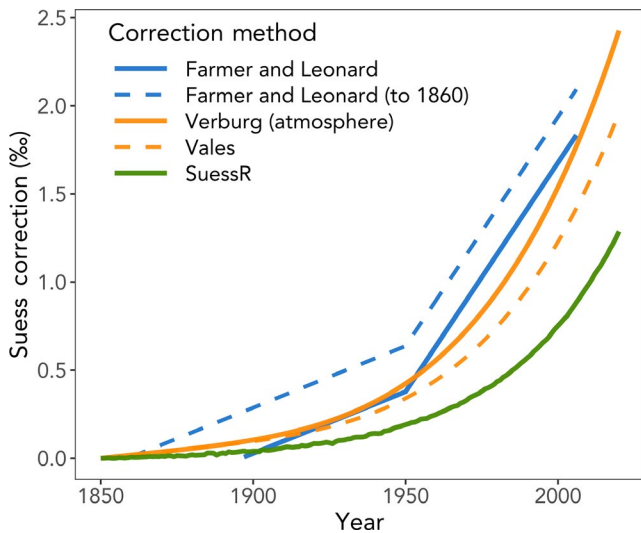
**FIGURE 1** Comparison of commonly used methods of Suess correction. Farmer and Leonard (2011) used a linear $\delta^{13}$C decline of −0.007‰ per year for samples collected from 1896 to 1950 and a further $\delta^{13}$C decline of −0.026‰ per year from 1951 to 2006 (solid blue). The dashed blue line shows the Farmer and Leonard correction applied back to 1860, the year they reference as the beginning of the yearly −0.007‰ decline. Verburg (2007) fit a sixth-order polynomial to a time series of atmospheric $\delta^{13}$C data to estimate the magnitude of the Suess effect in Lake Tanganyika (solid orange). Vales et al. (2020) added a 10-year lag to Verburg's equation and applied it to marine samples (dashed orange). The solid green line represents the net (combined Suess and Laws) corrections generated by SuessR for the Bering Sea. The shape and position of the SuessR correction in relation to the atmospheric line (solid orange) reflect the expected lag between the oceanic and atmospheric Suess effects, whereas the other approaches tend to overcorrect

SuessR package, thereby increasing the number of built-in regions available in future versions.

## 2 | BACKGROUND AND THEORY

### 2.1 | The Suess correction

Marine ecologists have used a variety of approaches to mathematically correct for the Suess effect. The magnitude of these corrections can vary widely, and a single approach often gains popularity within an individual sub-field (e.g. seabird research), making it more difficult to compare the results of studies performed on different taxa. The most basic Suess correction involves adding a fixed value (e.g. 1‰) to the $\delta^{13}$C values of modern samples to make them comparable to archaeological or historic specimens that lived prior to the Industrial Revolution (e.g. Conrad et al., 2018; Elliott Smith et al., 2020; Halffman et al., 2015; Newsome et al., 2004; Zangrando et al., 2016). This method of correction is simple and straightforward, but requires that modern samples represent a 'snapshot', rather than a time series, and that they be collected within a few years of one another. Furthermore, it requires a

good estimate of the magnitude of the Suess effect in the year(s) of sample collection. The use of a 1‰ correction by papers published as early as 2004 and as late as 2016 indicates that there is room for improvement in these estimates. To allow for comparison of samples collected at different times during the Industrial era, researchers have used linear estimates of the rate of change of $\delta^{13}$C values associated with the Suess effect, typically based on $\delta^{13}$C values of dissolved inorganic carbon (DIC) in a particular region or ocean basin (e.g. −0.018‰ per year across the entire North Atlantic basin; Quay et al., 2007), to calculate annual corrections (e.g. Espinasse et al., 2019; Matthews & Ferguson, 2014; Ramos et al., 2020; Rossman et al., 2013; Soto et al., 2018). An improved version of this approach incorporates an increase in the rate of $\delta^{13}$C decline after a specific year (e.g. 1950), to better approximate the exponential shape of the Suess effect curve (e.g. Alter et al., 2012; Bond & Lavers, 2014; Farmer & Leonard, 2011; Sun et al., 2019; Vokhshoori et al., 2019). Both of these methods allow for region-specific Suess corrections; however, there are also added complications. Researchers will typically correct all samples back to the first year of their time series (e.g. 1930) or forward to the last year (e.g. 2010), thereby generating the Suess corrected $\delta^{13}$C values that are comparable to one another, but not to pre-Industrial samples or to results produced from other studies that are corrected to a different year. When used to correct samples back to preindustrial $\delta^{13}$C levels (i.e. back to ~1850), these approaches tend to substantially overestimate the magnitude of the Suess effect (Figure 1), though they may produce more realistic corrections when applied to a restricted period of time.

Other Suess corrections have been generated using nonlinear models based on measured changes in environmental $\delta^{13}$C values. Researchers working in lakes have used higher-order polynomial models based on atmospheric trends to estimate the magnitude of the atmospheric Suess effect, assuming these systems are close to equilibrium with the atmosphere (e.g. Verburg, 2007). Some studies have applied these atmospheric corrections to marine systems by applying a lag to account for the incorporation of atmospheric $CO_2$ into surface waters (e.g. Vales et al., 2020), which is likely a better approximation of the Suess effect than provided by linear models; however, it is unclear whether the 10-year lag appropriately captures the disequilibrium between the atmospheric and oceanic Suess effect (Figure 1). Hilton et al. (2006) used values from the published literature to develop a more complex Suess correction, which accounts for the observed exponential decline in $\delta^{13}$C values of dissolved inorganic carbon in the global oceans associated with the absorption of anthropogenically produced $CO_2$. This correction also included a constant accounting for regional differences in $CO_2$ uptake by the ocean. Misarti et al. (2009) subsequently updated and adapted this correction for the Gulf of Alaska, and corrected an error in the original equation published by Hilton et al. (2006), where an addition symbol had been substituted for a multiplication symbol. The resulting equation (Misarti et al., 2009) is:

$$\text{Suess effect correction} = a \times e^{(b \times 0.027)}$$

In this equation, $a$ is a constant reflecting the maximum observed rate of $\delta^{13}C$ decline in surface waters DIC in a specific region, $b$ is the year of sample collection minus 1850 (the onset of the Industrial Revolution) and 0.027 is the parameter value obtained by Hilton et al. (2006) after fitting an exponential curve to the global ocean $\delta^{13}C$ data from 1945 to 1997 published by Gruber et al. (1999). The resulting Suess effect correction (a negative value) may then be subtracted from the uncorrected $\delta^{13}C$ data to obtain the Suess-corrected $\delta^{13}C$ value. This equation has since been used by numerous studies to calculate regional Suess corrections (e.g. Clark et al., 2019; Guiry et al., 2020; Harris et al., 2020; Kochi et al., 2018).

## 2.2 | The Laws correction

The second correction calculated and applied by SuessR was developed by Laws et al. (2002), and takes into account shifts in stable carbon isotope fractionation by phytoplankton associated with changes in water temperature, aqueous $CO_2$ concentrations and phytoplankton physiology. The equation for estimating the difference between aqueous $CO_2$ $\delta^{13}C$ values and those of the products of photosynthesis by phytoplankton (i.e. stable carbon isotope fractionation by phytoplankton, $\varepsilon_p$) is:

$$\varepsilon_p = \varepsilon_2 + \varepsilon_1 - \varepsilon_{-1} - \frac{1}{\left\{ 1 + \left[ [CO_2]_{aq} \times \frac{P}{\mu \times C \times (1+\beta)} \right] \right\}} \times \frac{(\varepsilon_2 - \varepsilon_{-1})}{(\beta + 1)}$$

In this equation, $\varepsilon_1$ represents the isotopic fractionation associated with diffusion of DIC into the cell, whereas $\varepsilon_{-1}$ represents the isotopic fractionation associated with diffusion of DIC out of the cell. Both of these terms are assumed to be constant at 1‰, and to cancel one another out (Laws et al., 2002); thus, their appearance at the beginning of the above equation serves primarily as a reminder of this assumption. The isotopic fractionation associated with carboxylation, represented in this equation by $\varepsilon_2$, is assumed to be constant at 26.5‰, the median of the values presented by Laws et al. (2002). $\beta$ is the ratio of net diffusional loss of $CO_2$ to carbon fixation, and is assumed to be constant. $P$ reflects the permeability of the plasmalemma (the plasma membrane which bounds the cell) to $CO_2$ ($p$) multiplied by the surface area of the cell (thus, $P = p \times$ cell surface area, with $p$ in m/day), $C$ the organic carbon content of the cell (in gC/cell) and $\mu$ is the average growth rate (in day$^{-1}$) of phytoplankton in a given region and year. Both $P$ and $C$ are proportional to cell size, with $P$ scaling to a cell's surface area and $C$ to cell volume. $[CO_2]_{aq}$ (in μmol/kg) represents the concentration of aqueous $CO_2$ in the seawater.

Estimates of $[CO_2]_{aq}$ are calculated by multiplying the estimated fugacity of the $CO_2$ in the ocean ($fCO_{2_{ocean}}$, in μatm) by the solubility of $CO_2$ in seawater at a given temperature and salinity ($K_0$). Calculating annual estimates of $fCO_{2_{ocean}}$ first requires comparing the regional rates of change of $fCO_{2_{atmosphere}}$ and $fCO_{2_{ocean}}$ to determine the proportion of atmospheric $CO_2$ concentration increase exhibited by the ocean in a given year. For example, if $fCO_{2_{atmosphere}}$ in a particular region increases by 10 μatm and $fCO_{2_{ocean}}$ by 6 μatm over the course of

a decade, the annual increase in surface seawater fugacity ($\Delta fCO_{2_{ocean}}$) for this region can be estimated by multiplying measured changes in $fCO_{2_{atmosphere}}$ ($\Delta fCO_{2_{atmosphere}}$) by 0.6. We refer to this number as the proportional rate of change ($C_p$). Annual estimates of $fCO_{2_{ocean}}$ can thus be calculated using the following equation:

$$fCO_{2_{ocean\,t+1}} = fCO_{2_{ocean\,t}} + \Delta fCO_{2_{atmosphere}} \times C_P$$

This approach requires an assumed starting value for $fCO_{2_{ocean}}$ at the beginning of the record ($fCO_{2_{ocean\,t=0}}$). Additionally, because records of atmospheric $CO_2$ concentrations are presented in parts per million (ppm), this approach assumes that $CO_2$ behaves as an ideal gas and that $fCO_{2_{atmosphere}}$ is directly proportional to atmospheric $CO_2$ concentrations. Annual estimates of $K_0$ can be generated using the following equation from Weiss (1974):

$$\ln(K_0) = A_1 + A_2 \times \left( \frac{100}{T} \right) + A_3 \times \ln \left( \frac{T}{100} \right)$$
$$+ SSS \times [B_1 + B_2 \times \left( \frac{T}{100} \right) + B_3 \times \left( \frac{T}{100} \right)^2]$$

In this equation, absolute temperature ($T$, in degrees Kelvin) and sea surface salinity (SSS), along with constants $A_{1-3}$ and $B_{1-3}$, are used to calculate the natural log of $K_0$ in ln(moles/l·atm). Once these terms have been calculated, they can be used to generate yearly estimates of $[CO_2]_{aq}$ using the following equation:

$$[CO_2]_{aq} = fCO_{2_{ocean}} \times K_0$$

To calculate the Laws correction, which is the overall change in $\varepsilon_p$ by phytoplankton since 1850, the estimated stable carbon isotope fractionation from 1850 is subtracted from that of the year in which a sample was collected:

$$\text{Laws correction} = \varepsilon_{p_{sampling\,year}} - \varepsilon_{p_{1850}}$$

Sea surface temperature (SST) and aqueous $CO_2$ concentrations have opposite effects on $\varepsilon_p$, with increases in SST leading to smaller $\varepsilon_p$ values, and increases in $[CO_2]_{aq}$ resulting in higher values for $\varepsilon_p$. Since 1850, increases in aqueous $CO_2$ concentrations have had more of an effect on $\varepsilon_p$ than have increasing water temperatures, and $\varepsilon_p$ has increased across the last ~170 years. Thus, the Laws correction is typically a positive number added to the sample's $\delta^{13}C$ value to account for this increase in $\varepsilon_p$ (because increasing $^{13}C$ fractionation through time means more negative $\delta^{13}C$ values in later years) and provide the Laws-corrected data.

## 3 | IMPLEMENTATION AND APPLICATION OF THE SuessR PACKAGE

### 3.1 | Overview of SuessR

Version 0.1.3 of SuessR includes four built-in regions for which users may calculate Suess and Laws corrections and apply them to their

data. These include three North Pacific regions (Bering Sea, Aleutian Islands, Gulf of Alaska; Figure 2; Table S1) and one North Atlantic region (Subpolar North Atlantic; Figure 2; Table S1). Additionally, the package includes the SuessR.custom() function, which allows users to supply their own regional parameters for the Suess and Laws Corrections. It is our hope that users will submit these data to the authors of the package for inclusion in future versions of SuessR. The updates to the equation used to generate the Laws correction and the introduction of the function for calculating the regional uptake constant for the Suess correction were primarily aimed at facilitating the process of using the SuessR package for custom regions. Users choosing to parameterize the Suess and Laws corrections for custom regions should have a thorough understanding of the physical, chemical and biological systems in the region of interest, and careful consideration is required to avoid erroneous results. Users intending to do so must make a number of important considerations pertaining to their region(s) of interest and the organisms sampled by their study. SuessR is available on CRAN (https://cran.r-project.org/web/packages/SuessR/index.html) and can be installed command 'install.packages('SuessR')' in the R console. A web-based Shiny app that allows users to interact with SuessR using a graphical user interface is also available (https://suessr.shinyapps.io/SuessR/).

## 3.2 | Calculation of the Suess correction

The SuessR package uses the equation developed by Hilton et al. (2006) and modified by Misarti et al. (2009), but introduces a different method for calculating the regional uptake constant $a$. To calculate this constant, the observed decline in DIC $\delta^{13}$C in a specific region over a given period is typically treated as a linear change and is divided by the number of years over which the change was observed, thus producing an annual rate of $\delta^{13}$C change. Taking the linear slope of an exponential curve will, however, produce substantially different results depending on which portion of the curve is used for the calculation. Thus, data from the same region will provide

different rates of $\delta^{13}$C change if data are examined from 1970 to 1979 and from 2000 to 2009, with the latter producing a larger annual change. To address this problem, the SuessR package contains a function that derives the regional uptake constant using a different approach. Because the observed change in $\delta^{13}$C DIC across a span of time closely approximates the magnitude of the Suess effect across that period, we can solve for the regional uptake constant using the Suess correction equation as follows:

$$\text{Suess effect}_{\text{Year 1}} = a \times e^{(b_1 \times 0.027)}$$

$$\text{Suess effect}_{\text{Year 2}} = a \times e^{(b_2 \times 0.027)}$$

$$\text{Observed change in } \delta^{13}C_{\text{DIC}_{\text{Year 2 - Year 1}}} = \text{Suess effect}_{\text{Year 2}} - \text{Suess effect}_{\text{Year 1}}$$

$$\text{Observed change in } \delta^{13}C_{\text{DIC}_{\text{Year 2 - Year 1}}} = a \times e^{(b_2 \times 0.027)} - a \times e^{(b_1 \times 0.027)}$$

$$a = \frac{\text{Observed change in } \delta^{13}C_{\text{DIC}_{\text{Year 2 - Year 1}}}}{\left( e^{(b_2 \times 0.027)} - e^{(b_1 \times 0.027)} \right)}$$

In this way, the regional uptake constant for any body of water can be calculated using observed changes in $\delta^{13}C_{\text{DIC}}$ from any time period. This approach assumes that the regional uptake constant for a given body of water has remained the same since 1850. Once this term has been estimated, calculating and applying the Suess correction is straightforward.

The regional uptake constants used for SuessR's built-in regions include an update to those used by Misarti et al. (2009) for the North Pacific and a new estimate for the subpolar North Atlantic. Watanabe et al. (2011) estimated the oceanic Suess effect in the subpolar North Pacific to have a linear rate of $\delta^{13}C_{\text{DIC}}$ decline of –0.019‰ per year between 1997 and 2006. Using the above equation to solve for $a$ results in a regional uptake constant of –0.013. In the subpolar North Atlantic, interpretation of observed $\delta^{13}C_{\text{DIC}}$ declines is complicated by changes in water mass properties (Quay et al., 2007); however, Quay et al. (2007) estimated a decline of –0.017‰ per year between
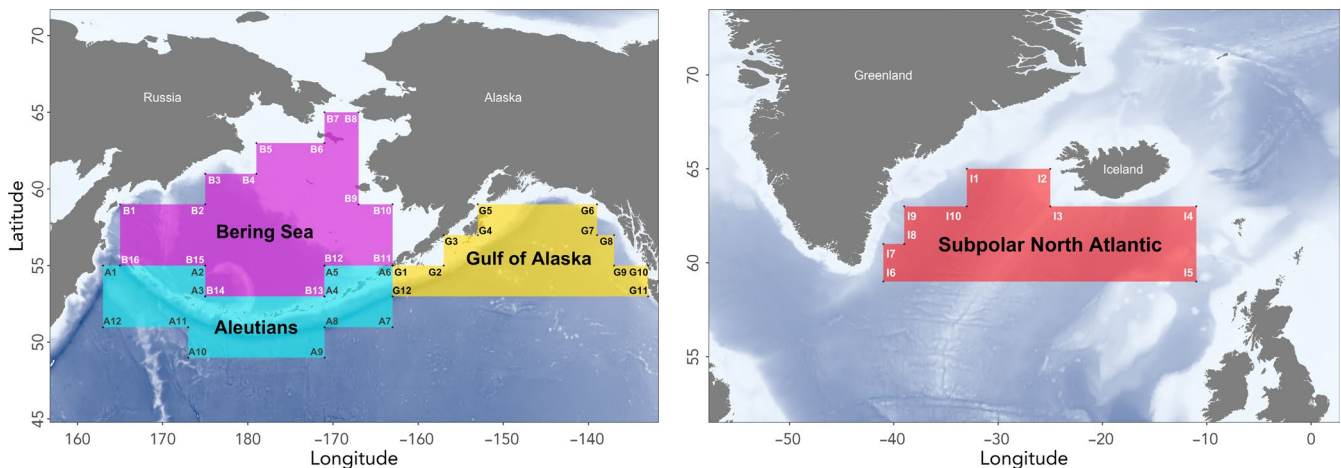


**FIGURE 2** Map of regions built into version 0.1.3 of SuessR: Bering Sea, Aleutian Islands, Gulf of Alaska and Subpolar North Atlantic. Coordinates of polygon corners are listed in Table S1

1993 and 2003 using an isopycnal multiple linear regression, which matched well with other estimates from the North Atlantic. This estimate yields a regional uptake constant of –0.013. The identical values calculated for the subpolar North Pacific and subpolar North Atlantic seem reasonable, given that the majority of the variation in the Suess effect in the surface ocean is associated with latitude (Eide et al., 2017; Quay et al., 2003, 2007), although there are some indications that the Suess effect may be slightly more pronounced in the subpolar North Atlantic (Eide et al., 2017).

## 3.3 | Calculation of the Laws correction

Using reconstructions and records of annual atmospheric $CO_2$ concentrations, sea surface temperature (SST) and sea surface salinity (SSS), yearly estimates of regional aqueous $CO_2$ concentrations can be generated back to 1850. These data were compiled from various gridded global datasets, using version 0.4.8 of the RERDDAPXTRACTO package in R (Mendelssohn, 2020). SST data were taken from the Extended Reconstructed Sea Surface Temperature (ERSST) v5 dataset (Huang et al., 2017; https://www.ncdc.noaa.gov/data-access/marineocean-data/extended-reconstructed-sea-surface-temperature-ersst-v5). This dataset extends from AD 1854 to present, and provides global monthly SST estimates in a 2° × 2°grid. The mean annual SSTs from 1854 to 1864 were used to approximate the SST for the years from 1850 to 1853. It should be noted that the gridded values extend from 88°S to 88°N, and are centred on the even values such that the grid point at 50°N and 160°W extends from 49°N to 51°N and from 159°W to 161°W. The spatial scale of the 2° × 2° grid was a determining factor in the delineation of the built-in regions included in the SuessR package (Figure 2; Table S1). Sea surface salinity (SSS) was compiled from two datasets. Version 2.2.4 of the Simple Ocean Data Assimilation (SODA) contains monthly mean salinity estimates for 1871 to 2010 on a 0.5° × 0.5° grid (Giese & Ray, 2011; https://iridl.ldeo.columbia.edu/SOURCES/.CARTON-GIESE/.SODA/.v2p2p4/?Set-Language=en). Annual means for the period from 1850 to 1870 were approximated using the mean SSS estimates for 1871 to 1890. For 2011 and later, salinity data were taken from version 6.6.2 of the Microwave Imaging Radiometer using Aperture Synthesis (MIRAS) Soil Moisture and Ocean Salinity (SMOS) dataset (Sea Surface Salinity-Near Real Time-MIRAS SMOS, 2020; https://coastwatch.noaa.gov/cw/satellite-data-products/sea-surface-salinity/miras-smos.html). These data are gridded at 0.25° × 0.25° and are available as a 3-day mean. Annual mean salinity estimates were calculated for the regions included in the SuessR package. Some mismatch may exist between the SODA and MIRAS SMOS salinity estimates; however, these are typically small and result in negligible differences in the overall Laws correction. These datasets were selected because their spatial scale is global and they contain gridded data. Thus, users wishing to apply Suess and Laws corrections to data from regions not built into the package will be able to extract SST and SSS data for their region of interest from these same data sources.

Atmospheric $CO_2$ concentrations (in ppm) from 1850 to 2020 were downloaded from the Scripps $CO_2$ program (https://scrippsco2.ucsd.edu/). This dataset compiles reconstructed $CO_2$ concentration estimates from ice cores (prior to 1958), and measurements taken at Mauna Loa, Hawaii, and the South Pole (1958–present), to create a merged, yearly global $CO_2$ record (Keeling et al., 2005; MacFarling Meure et al., 2006). Atmospheric $CO_2$ concentrations were then used to produce yearly estimates of $[CO_2]_{aq}$ using the equations in Section 2.2 of this paper. For these calculations, the initial $fCO_{2_{ocean}}$ was assumed to be 285.78 ppm, the mean estimate of atmospheric $CO_2$ concentrations for the years 1940–1949. Estimates of the proportional rate of change of $fCO_{2_{ocean}}$ in relation to $fCO_{2_{atmosphere}}$ were calculated using regional data from the Surface Ocean $CO_2$ Atlas (SOCAT; Bakker et al., 2016, https://www.socat.info/index.php/data-access/) and the rate of $fCO_{2_{atmosphere}}$ increases in the Northern Hemisphere. Given relative sparsity of $fCO_{2_{ocean}}$ data in both time and space, $\Delta fCO_{2_{ocean}}$ was calculated by fitting linear regressions to yearly $fCO_{2_{ocean}}$ from 1970s to 2010s (Pacific: 1970, 1973–1980, 1982–1983, 1985–2019; Atlantic: 1981–1982, 1989–2019), for a broad area in the subpolar North Pacific (from 45° to 65° latitude and 150° to –130° longitude) and subpolar North Atlantic (from 45° to 70° latitude and –60° to 0° longitude). This resulted in a 1.57 μatm/year increase in the subpolar North Pacific, and a 1.74 μatm/year increase in the subpolar North Atlantic. Rates of $fCO_{2_{atmosphere}}$ increase were calculated for each of the built-in regions using the methods outlined in Wang et al. (2016), with parameters from Weiss (1974) and Weiss and Price (1980). For these calculations, sea level pressure (SLP) data were downloaded from the ERA5 dataset (https://www.ecmwf.int/en/forecasts/datasets/reanalysis-datasets/era5), and dry air $CO_2$ data ($xCO_2$) from the National Oceanographic and Atmospheric Administration (NOAA) Marine Boundary Layer (MBL) Reference dataset (https://www.esrl.noaa.gov/gmd/ccgg/mbl/data.php). Previously downloaded SST and SSS data from the ERSST v5, SODA and MIRAS SMOS datasets were also used. Calculated $fCO_{2_{atmosphere}}$ values were then summarized to yearly averages from 1979 to 2018, and used to calculate a regional rate of $fCO_{2_{atmosphere}}$ increase. This resulted in a rate of increase of 1.78, 1.78 and 1.77 μmol/year for the Bering Sea, Aleutian Islands and the Gulf of Alaska, respectively. This yielded a proportional rate of change of 0.88 for the Bering Sea and Aleutian Islands, and 0.89 for the Gulf of Alaska. The calculated rate of $fCO_{2_{atmosphere}}$ increase for the Subpolar North Atlantic was 1.74 μmol/year; thus, the observed rate of increase for $fCO_{2_{ocean}}$ was equal to that of the atmosphere. This region of the North Atlantic has experienced changes in water mass properties that has led to $fCO_{2_{ocean}}$ increases that are unrelated to uptake of $CO_2$ from the atmosphere (Quay et al., 2007; Schuster et al., 2009), introducing a confounding factor into these analyses. Although the proportion of atmospheric $CO_2$ increase exhibited by the surface ocean could not be directly estimated for this region, the calculated value of 1.00 in the Subpolar North Atlantic was likely only slightly higher than the actual value, given the similar magnitudes of previous estimates of the Suess effect in the Subpolar North Pacific and Atlantic (Eide et al., 2017; Quay et al., 2007). This indicates that the true $C_p$ for

the Subpolar North Atlantic was likely somewhere between ~0.88 and 1.00. To be conservative, the calculated value ($C_p$ = 1.00) was used for this region, which matches with reports that $CO_2$ concentrations in North Atlantic surface waters are increasing at about the same rate as the atmosphere (Eide et al., 2017). It is possible that apparent changes in $fCO_{2_{ocean}}$ in other regions may also be confounded by changes in water mass properties, and this possibility should be considered when supplying data for custom regions to SuessR. Such changes are typically reported and discussed in the literature, and often manifest as differences between modelled and observed values for rates of $\delta^{13}C_{DIC}$ change in surface waters.

The SuessR package uses the equation for calculating $\varepsilon_p$ from Laws et al. (2002) as the framework for estimating the Laws correction; however, some components have been updated or amended to make using this equation simpler and to better approximate phytoplankton communities, as opposed to individual species. One of these updated pieces is a different approach for calculating the organic carbon content of the cell, $C$, than that originally referenced by Laws et al. (2002). This calculation, from Menden-Deuer and Lessard (2000), estimates $C$ based on cell radius, $r$. The incorporation of this new correction means that only the average cell radius, $r$ (in $\mu$), needs to be supplied to SuessR, simplifying the process for users to generate calculations using data appropriate to their region of interest. To most closely approximate the organic carbon content of the phytoplankton community, SuessR uses the equation $C\left(pg \cdot cell^{-1}\right) = 0.216 \times$ cell volume$^{0.939}$, where cell volume is measured in $\mu^3$. This assumes a taxonomically diverse group of protist phytoplankton, but excludes large diatoms with cell volumes >3,000 μm$^3$. Researchers specifically studying diatoms, dinoflagellates or food webs based primarily on these groups might prefer to use the relationship between organic carbon content and cell size specific to these groups, as reported by Menden-Deuer and Lessard (2000); however, SuessR currently does not support the use of these equations, and the Laws correction would need to be calculated manually. For the majority of phytoplankton communities, however, the equation employed by SuessR should adequately approximate $C$. Hilton et al. (2006) and Misarti et al. (2009) assumed an average cell radius of 10 μ; however, estimates of phytoplankton size distributions from the published literature indicate that this is likely too large to be representative of the average cell size across most phytoplankton communities (e.g. Acevedo-Trejos et al., 2014; Bolaños et al., 2020; Laney & Sosik, 2014; Marañón, 2015; Polovina & Woodworth, 2012). To better approximate a community average, and to incorporate the nanoplankton and picoplankton that make up a large proportion of phytoplankton biomass, SuessR uses an average cell radius of 5 μ for the built-in regions in the subpolar North Pacific and North Atlantic. This number is supported by the published literature and appears to be a good approximation of the average community cell size in subpolar environments (Bolaños et al., 2020). As with the equation for calculating cell volume, researchers focusing on a food web based on larger or smaller phytoplankton could choose to improve the accuracy of their Laws corrections by supplying a different average cell radius to SuessR using the *SuessR.custom()* function.

In addition to the new value for $r$ and the updated calculation for $C$, SuessR also incorporates a method for calculating phytoplankton community growth rate estimates, $\mu$, based on sea surface temperature (SST). The equation for the relationship between SST and $\mu$ comes from the following Q10 model, as parameterized by Sherman et al. (2016), and allows growth rate estimates to shift in response to changes in SST since 1850:

$$\mu = 0.89 \times 1.47^{\frac{T-303.15}{10}}$$

In this equation, $T$ represents SST (in degrees Kelvin). As with the updated calculation for $C$, this new equation for estimating $\mu$ reduces the number of parameters required by the Laws correction, thus simplifying the process of supplying custom data to calculate corrections for regions not built into the SuessR package.

Because both $C$ and $P$ scale in relation to the radius of the cell, cell size plays a critical role in determining the magnitude of the overall Laws correction. A sensitivity analysis was conducted to examine the impact that each parameter in the Laws equation had on the magnitude of the overall Laws correction, given a small (1 μ), medium (5 μ) and large (10 μ) cell radius (Figure 3). For this analysis, $p$ (from $P = p \times$ cell surface area), $\beta$, SST and $[CO_2]_{aq}$ were each allowed to vary while the others were held constant. Random values for the varying parameter were sampled from a normal or gamma distribution with a mean and variance based on estimates from the published literature (Table S2), and the others were held constant at their means. The resulting values were then supplied as parameters to the Laws equation to calculate an estimate of phytoplankton $^{13}C$ fractionation ($\varepsilon_p$). This process was repeated 10,000 times for each cell radius (1 μ, 5 μ and 10 μ). The $\varepsilon_p$ values that resulted from varying each parameter were then plotted (Figure 3). For all parameters, the magnitude of the observed differences increased with increasing cell size. At a radius of 1 μ, none of the parameters produced substantial differences in the overall $\varepsilon_p$ when varied. At 10 μ, these differences were much larger, and if allowed to vary together, would be expected to compound one another. Finally, the analysis was repeated with all parameters allowed to vary independently.

The results of the sensitivity analysis are important to the interpretation and application of the Laws correction. Varying $[CO_2]_{aq}$ and SST resulted in moderate changes to $\varepsilon_p$, whereas varying $\beta$ had little effect on this value (Figure 3). The effects of $[CO_2]_{aq}$ and SST were expected, as they were the primary reason for calculating $\varepsilon_p$. Increasing $[CO_2]_{aq}$ resulted in larger $\varepsilon_p$ values, whereas increasing SST resulted in smaller values for $\varepsilon_p$. The sensitivity analysis also indicated that $\varepsilon_p$ is strongly impacted by changes in cell size, which not only changes the calculated value of $\varepsilon_p$ (larger cells = lower $\varepsilon_p$ values) but also compounds the effects of varying the other parameters. Hilton et al. (2006) used a cell radius of 10 μ to estimate the Laws correction parameters, and this value was carried forward by Misarti et al. (2009). The sensitivity analyses revealed that cell radius interacts with each of the other variables in the equation, with larger cell sizes resulting in a greater change in $\varepsilon_p$ when each of the other parameters is allowed to vary (Figure 3). The greater variability at larger
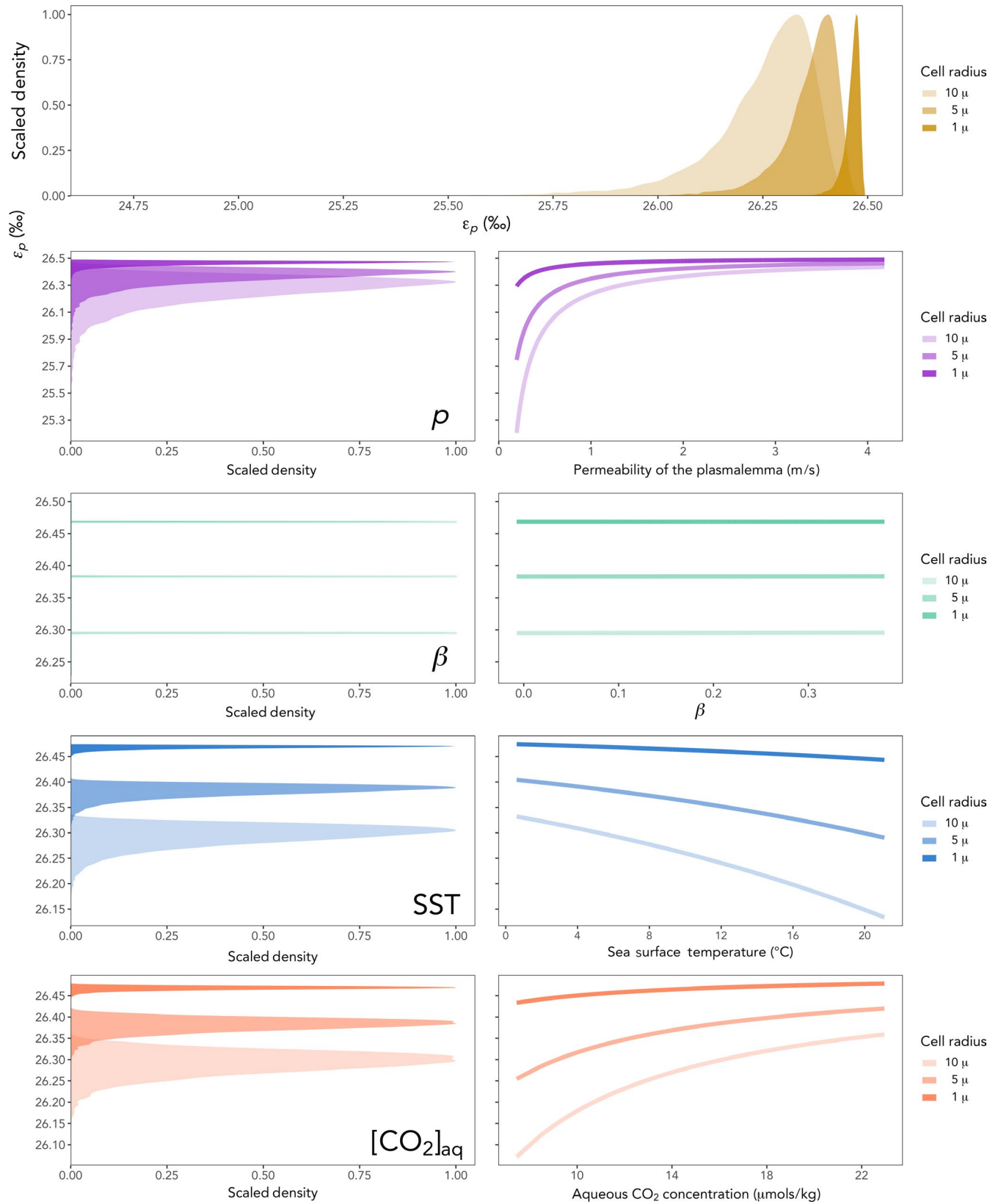
**FIGURE 3** Results of the sensitivity analyses of the Laws correction parameters. Top panel presents the distribution of $\varepsilon_p$ (‰) at three different cell radii (10 μ—lightest shade, 5 μ—medium shade and 1 μ—darkest shade) when all parameters ($p$, $\beta$, SST and $[CO_2]_{aq}$) were varied independently. Bottom panels show the distribution when only one parameter was varied (left panels, top to bottom: $p$, $\beta$, SST, and $[CO_2]_{aq}$) and lines depicting the relationship between the output data and the input values for each parameter when other parameters were held constant (right panels, same order). Means and standard deviations of the distributions from which input values were drawn are presented in Table S2

cell sizes is most apparent in the scenario in which all parameters are allowed to vary, with small cells exhibiting almost no variability in $\varepsilon_p$, and large cells varying much more widely. Thus, selecting an average cell radius that best characterizes the phytoplankton communities responsible for the bulk of the primary production in the region of interest is the most important consideration when selecting variables to estimate Laws corrections for a new region. Although published estimates of size distributions within phytoplankton communities are becoming more common in recent years (e.g. Acevedo-Trejos et al., 2014; Bolaños et al., 2020; Laney & Sosik, 2014; Marañón, 2015; Polovina & Woodworth, 2012), there is currently a dearth of empirical data for estimating average cell radius, and more research is needed to better characterize phytoplankton cell size distributions.

The term describing the permeability of the plasmalemma to $CO_2$, $p$, adds additional complications to calculating the Laws correction. The overall carbon fractionation, $\varepsilon_p$, is highly sensitive to changes in $p$ (Figure 3). As $p$ approaches zero, the calculated $\varepsilon_p$ values rapidly decline, particularly for larger cells. In their original calculations, Laws et al. (2002) used $1 \times 10^{-5}$ m/s, as a 'working mean' of the maximum and minimum literature values. Note the difference in units between literature references to $p$ (m/s), and the units required for the Laws correction (m/day). For SuessR's calculations, the value chosen for $p$ ($1.5 \times 10^{-5}$ m/s = 1.296 m/day) is the median of 27 estimates of $p$ from the published literature (Table S3). This value is on the cusp of the sharp declines in $\varepsilon_p$ visible in Figure 3 that resulted from small decreases in the value of $p$. The fact that it is slightly larger than the value used by Hilton et al. (2006) and Misarti et al. (2009) is responsible, in part, for the smaller Laws corrections calculated by SuessR, as compared to these two papers. The value used by SuessR is calculated using data from a variety of phytoplankton groups and is likely a good representation of a community average value for $p$. That said, the sensitivity of the Laws correction to $p$, as well as the relative lack of understanding of the natural variability in this term, suggests that it warrants further research. Many of the smaller $p$ values in the published literature (Table S3) would result in unrealistic estimates of $\varepsilon_p$, and models suggest that values of $p$ substantially smaller than $1 \times 10^{-4}$ m/s are unlikely to be representative of marine phytoplankton species that rely primarily on diffusive uptake of $CO_2$ (Rau et al., 1996). Future research that generates a better understanding of $p$ will help to constrain this term, and may provide a more realistic estimate of the average $p$ across phytoplankton communities for use in calculating the Laws correction.

## 3.4 | Example application

The SuessR package contains three functions. *SuessR()* calculates Suess and Laws corrections for samples collected in one of the four built-in regions. *SuessR.custom()* allows users to correct $\delta^{13}C$ data from a region not built into the SuessR package by supplying the region-specific parameters required to calculate the corrections. The *reg.uptake()* function allows users to calculate the regional uptake constant ('$a$' from the

**TABLE 1** Example input dataset for the *SuessR()* or *SuessR.custom()* functions. Columns must include sample id, year of sample collection, region of sample collection and uncorrected $\delta^{13}C$ data (in ‰), named 'id', 'year', 'region' and 'd13c', respectively. Note that the *SuessR.custom()* function also requires the user to supply region-specific data of the type included in the built-in reference dataset SuessR.reference.data; Supplementary Dataset SD1)

| Id | Year | Region | d13c |
| --- | --- | --- | --- |
| Sample 001 | 1945 | Aleutian Islands | −13.8 |
| Sample 002 | 1973 | Aleutian Islands | −14.5 |
| Sample 003 | 1988 | Aleutian Islands | −13.0 |
| Sample 004 | 2001 | Aleutian Islands | −12.9 |
| Sample 005 | 2010 | Aleutian Islands | −15.2 |
| Sample 006 | 1895 | Subpolar North Atlantic | −14.6 |
| Sample 007 | 1953 | Subpolar North Atlantic | −14.5 |
| Sample 008 | 1965 | Subpolar North Atlantic | −14.2 |
| Sample 009 | 1999 | Subpolar North Atlantic | −14.0 |
| Sample 010 | 2007 | Subpolar North Atlantic | −13.7 |

Suess correction equation, and 'up.con' in the SuessR.reference.data file, Supporting Information Dataset SD1) for a particular region based on empirical measurements of $\delta^{13}C_{DIC}$ changes (proxy for the magnitude of the Suess effect) from that region. Data supplied to SuessR for corrections must follow a specific format for use by the package. These data files must contain a column for the sample ID ('id'), year of sample collection ('year'), region of sample origin ('region') and the uncorrected $\delta^{13}C$ data ('d13c'), otherwise an error is returned. Table 1 contains an example dataset with 10 samples from two regions.

Once the data have been loaded into R, the *SuessR()* function can be used to calculate the Suess and Laws corrections and apply them to the uncorrected $\delta^{13}C$ data. This function uses the built-in reference dataset (SuessR.reference.data; Supporting Information Dataset SD1) to calculate and apply the corrections. It references the region and year provided for each sample, so samples from different regions and periods can be corrected simultaneously. Upon completion, SuessR returns the results for each sample, which include the uncorrected $\delta^{13}C$ data ('d13c.uncor'), the Suess correction ('Suess.cor'), the Laws correction ('Laws.cor'), the net correction ('net.cor') and the corrected $\delta^{13}C$ data ('d13c.cor'; Table 2). The Suess.R() function also includes an optional argument 'correct.to' with a default of 1850 to correct for the entire Suess effect since the Industrial Revolution; however, some users may want to correct $\delta^{13}C$ data to a specific year, rather than back to preindustrial values. For example, a user analysing a dataset of $\delta^{13}C$ values spanning the years 1980–2000 might only want to correct for the Suess effect after 1980, or might want to correct samples forward to the year 2000 to make their data comparable. The 'correct.to' argument allows users to specify a year to which the data should be corrected.

| Id | Year | d13c. uncor | Laws.cor | Suess.cor | net.cor | d13c. cor |
|---|---|---|---|---|---|---|
| Sample 001 | 1945 | –13.8 | 0.006 | 0.156 | 0.162 | –13.638 |
| Sample 002 | 1973 | –14.5 | 0.016 | 0.347 | 0.363 | –14.137 |
| Sample 003 | 1988 | –13.0 | 0.021 | 0.527 | 0.548 | –12.452 |
| Sample 004 | 2001 | –12.9 | 0.025 | 0.754 | 0.778 | –12.122 |
| Sample 005 | 2010 | –15.2 | 0.028 | 0.964 | 0.993 | –14.207 |
| Sample 006 | 1895 | –14.6 | 0.001 | 0.031 | 0.031 | –14.569 |
| Sample 007 | 1953 | –14.5 | 0.010 | 0.197 | 0.206 | –14.294 |
| Sample 008 | 1965 | –14.2 | 0.012 | 0.277 | 0.289 | –13.911 |
| Sample 009 | 1999 | –14.0 | 0.031 | 0.713 | 0.744 | –13.256 |
| Sample 010 | 2007 | –13.7 | 0.030 | 0.888 | 0.919 | –12.781 |

**TABLE 2** Output from the *SuessR()* function when supplied the example input data from Table 1. Columns include sample id ('id'), year of sample collection ('year'), uncorrected $\delta^{13}C$ data ('d13c. uncor', in ‰), the magnitude of the estimated Laws correction ('Laws.cor', in ‰), the magnitude of the estimated Suess correction ('Suess.cor', in ‰), the magnitude of the estimated net correction ('net.cor', in ‰) and the corrected $\delta^{13}C$ data ('d13c.cor', in ‰)

When publishing $\delta^{13}C$ data corrected by SuessR, it will be important to make clear the year to which the data have been corrected.

SuessR contains an additional function, *SuessR.custom()*, which allows users to supply their own regional parameters for the Suess and Laws corrections. These supplied parameters are appended to the built-in SuessR.reference.data (Supplementary Dataset SD1) and must be supplied in the same format. To input data for a custom region, the user must first create a data frame with the regional parameters for the Suess and Laws corrections. This data frame can then be called using the 'custom.region.data' argument in the *SuessR.custom()* function. The name of the custom region should be specified in the 'region' column of the data frame, and this region must be specified when $\delta^{13}C$ values for this region are supplied for correction. Because the parameters chosen will determine the final values for the Suess and Laws corrections, it is critical that they are carefully selected and vetted before being supplied to SuessR. It is the authors' hope that users will submit the parameters for their custom regions along with the associated references to be incorporated as built-in regions in future versions of SuessR. These custom data can be submitted to the corresponding author of this paper or to the maintainer of the SuessR package, as laid out in the package documentation.

The *reg.uptake()* function is used to calculate the regional uptake constant for a region, which can be supplied to the *SuessR.custom()* function as part of the 'custom.region.data' object. This function requires three arguments: 'year1', 'year2' and 'd13c.change'. The term 'year1' indicates the calendar year in which the first $\delta^{13}C_{DIC}$ observation was made, whereas 'year2' is the year in which the last $\delta^{13}C_{DIC}$ measurement was taken. 'd13c.change' represents the magnitude of change in $\delta^{13}C_{DIC}$ (in ‰) observed between those years. Because of the potential biases and problems associated with snapshot estimates of $\delta^{13}C_{DIC}$, many of the more current studies in the published literature use a multiple linear regression approach to estimating the change in $\delta^{13}C_{DIC}$ through time (Quay et al., 2007). This method more effectively separates natural and anthropogenic $\delta^{13}C_{DIC}$ changes by accounting for seasonal variability in $\delta^{13}C_{DIC}$, and predicts $\delta^{13}C_{DIC}$ using measured hydrographic data. The regressions typically provide a linear approximation of $\delta^{13}C_{DIC}$ changes (e.g. –0.018‰ per year

from 1990 to 2000). In this example, 'year1' would be 1990, 'year2' would be 2000 and d13c.change would be –0.198‰ (–0.018‰ $year^{-1} \times 11$ year). The resulting regional uptake constant would be $a = -0.015$.

## 4 | CONCLUSIONS

The SuessR package provides a widely accessible, customizable and easy to use tool that allows ecologists to apply corrections to account for the influence of anthropogenic $CO_2$ on marine $\delta^{13}C$ data. For samples collected in 2020, SuessR estimates a net correction of 1.29‰ for the Bering Sea, 1.30‰ for the Aleutian Islands and Gulf of Alaska, and 1.31‰ for the Subpolar North Atlantic. The corrections produced by SuessR align well with recent literature estimates of the magnitude of the Suess effect since the preindustrial era (Eide et al., 2017), and the shape of the Suess correction curve closely follows the independently generated atmospheric curve published by Verburg (2007), with the expected offset between changes in atmospheric and oceanic $\delta^{13}C$ values (Figure 1). The exponential nature of the Suess effect, coupled with a greater recognition of the importance of long-term datasets in ecological research, mean that the application of Suess corrections is no longer just a problem faced by archaeologists, palaeoecologists and historical ecologists. In contrast, the output of the updated Laws equation implemented by SuessR indicates that temperature- and $CO_2$-related changes in fractionation by marine phytoplankton are less important than previously thought, although this may apply only to the subpolar regions built into the package, and not at lower latitudes (Young et al., 2013). The results of some studies indicate that increasing temperature and $CO_2$ concentrations might cause much larger changes in stable carbon isotope fractionation by marine phytoplankton ($\varepsilon_p$) than predicted by SuessR (Cullen et al., 2001; Young et al., 2013), due primarily to the use of different methods of calculating $\varepsilon_p$. Further study is merited to determine which approach better characterizes marine phytoplankton communities, and some updates to SuessR may be required in the future if another method of calculation is found to be more accurate. Improvements and updates to future releases of

SuessR will rely, in part, on better constraints on model parameters, including $r$ (the average community cell radius) and $p$ (the permeability of the plasmalemma to $CO_2$), which are particularly important to improving the Laws correction. Future versions of the Laws correction might be improved using an iterative process to draw cell sizes from a distribution representing a phytoplankton community, rather than summarizing the community to a single mean value. Similarly, an update to the long-term changes in $\delta^{13}C_{DIC}$ modelled by Gruber et al. (1999) will be important to verify that the original Suess correction equation published by Hilton et al. (2006) is still an adequate characterization of the magnitude of the oceanic Suess effect. Furthermore, as some areas of the surface ocean become saturated with $CO_2$, the dynamics of the oceanic Suess effect will change in ways that are not currently characterized by the Suess correction. As with any data correction approach, it is important to consider the possibility of bias or error within the correction itself, and presenting both the uncorrected and corrected data is strongly encouraged. This allows researchers and subsequent users of the data to assess the impacts of applying the correction, and to explore alternate hypotheses for observed variability in stable carbon isotope values. Despite these uncertainties and ways in which the Suess and Laws corrections may be refined in the future, the corrections produced by SuessR match with reported estimates of the magnitude of the Suess effect in the surface ocean. This tool has the potential to improve future research by providing a unified approach to calculating and applying Suess corrections for marine $\delta^{13}C$ data, that is easy to access and free to use. Furthermore, submission of compiled regional environmental data by users will allow for more built-in regions to be added in future versions of SuessR, further increasing its ease of use. Custom regional data can be submitted to the corresponding author or to the SuessR maintainer as designated in the package's documentation.

## ACKNOWLEDGEMENTS

## AUTHORS' CONTRIBUTIONS

C.T.C., M.R.C., B.P.F., N.M. and M.D.S. adapted the Suess and Laws corrections for use by SuessR; M.R.C. performed the pCO$_2$ calculations; C.T.C. and M.R.C. conducted the sensitivity analyses; C.T.C. and F.J.M. wrote the R package and Shiny App; C.T.C., M.R.C., B.P.F., F.J.M., N.M. and M.D.S. wrote the manuscript.

## PEER REVIEW

The peer review history for this article is available at https://publons.com/publon/10.1111/2041-210X.13622.

## DATA AVAILABILITY STATEMENT

All data used by SuessR are publicly available in online repositories as specified in the text and references. These datasets include ERSST v5 (SST; https://www.ncdc.noaa.gov/data-access/marineocean-data/extended-reconstructed-sea-surface-temperature-ersst-v5), SODA 2.2.4 (SSS; https://iridl.ldeo.columbia.edu/SOURCES/.CARTON-GIESE/.SODA/.v2p2p4/?Set-Language=en), MIRAS SMOS (SSS; https://coastwatch.noaa.gov/cw/satellite-data-products/sea-surface-salinity/miras-smos.html), the Scripps $CO_2$ program ([CO$_2$]$_{atm}$; https://scrippsco2.ucsd.edu/), SOCAT ($f$CO$_{2ocean}$; https://www.socat.info/index.php/data-access/), ERA5 (SLP; https://www.ecmwf.int/en/forecasts/datasets/reanalysis-datasets/era5) and NOAA MBL ($x$CO$_2$; https://www.esrl.noaa.gov/gmd/ccgg/mbl/data.php). SuessR documentation can be found on CRAN (https://cran.r-project.org/web/packages/SuessR/index.html) and code for functions can be accessed in the R console.

## ORCID

*Casey T. Clark* https://orcid.org/0000-0002-6311-9768
*Mattias R. Cape* https://orcid.org/0000-0002-5621-1128
*Mark D. Shapley* https://orcid.org/0000-0003-4770-1878
*Franz J. Mueter* https://orcid.org/0000-0001-6320-4164
*Bruce P. Finney* https://orcid.org/0000-0002-2639-6512
*Nicole Misarti* https://orcid.org/0000-0003-2232-0964

## REFERENCES

Acevedo-Trejos, E., Brandt, G., Steinacher, M., & Merico, A. (2014). A glimpse into the future composition of marine phytoplankton communities. *Frontiers in Marine Science*, *1*(15), 1–12. https://doi.org/10.3389/fmars.2014.00015

Alter, S. E., Newsome, S. D., & Palumbi, S. R. (2012). Pre-whaling genetic diversity and population ecology in eastern pacific gray whales: Insights from ancient DNA and stable isotopes. *PLoS One*, *7*(5), 1–12. https://doi.org/10.1371/journal.pone.0035039

Bacastow, R. B., Keeling, C. D., Lueker, T. J., Wahlen, M., & Mook, W. G. (1996). The $^{13}$C Suess effect in the world surface oceans and its implications for oceanic uptake of $CO_2$: Analysis of observations at Bermuda. *Global Biogeochemical Cycles*, *10*(2), 335–346. https://doi.org/10.1029/96GB00192

Bakker, D. C. E., Pfeil, B., Landa, C. S., Metzl, N., O'Brien, K. M., Olsen, A., & Xu, S. (2016). A multi-decade record of high-quality $f$CO$_2$ data in version 3 of the Surface Ocean $CO_2$ Atlas (SOCAT). *Earth System Science Data*, *8*(2), 383–413. https://doi.org/10.5194/essd-8-383-2016

Bolaños, L. M., Karp-Boss, L., Choi, C. J., Worden, A. Z., Graff, J. R., Haëntjens, N., Chase, A. P., Della Penna, A., Gaube, P., Morison, F., Menden-Deuer, S., Westberry, T. K., O'Malley, R. T., Boss, E., Behrenfeld, M. J., & Giovannoni, S. J. (2020). Small phytoplankton dominate western North Atlantic biomass. *The ISME Journal*, *14*(7), 1663–1674. https://doi.org/10.1038/s41396-020-0636-0

Bond, A. L., & Lavers, J. L. (2014). Climate change alters the trophic niche of a declining apex marine predator. *Global Change Biology*, *20*(7), 2100–2107. https://doi.org/10.1111/gcb.12554

Clark, C. T., Horstmann, L., de Vernal, A., Jensen, A. M., & Misarti, N. (2019). Pacific walrus diet across 4000 years of changing sea ice conditions. *Quaternary Research*, 1–17. https://doi.org/10.1017/qua.2018.140

Conrad, C., Barceló, L. P., Seminoff, J. A., Tomaszewicz, C. T., Labonte, M., Kemp, B. M., Jones, E. L., Stoyka, M., Bruner, K., & Pastron, A. (2018). Ancient DNA analysis and stable isotope ecology of sea turtles (Cheloniidae) from the gold rush-era (1850s) eastern Pacific Ocean. *Open Quaternary*, *4*(3), 1–13. https://doi.org/10.5334/oq.41

Cullen, J. T., Rosenthal, Y., & Falkowski, P. G. (2001). The effect of anthropogenic $CO_2$ on the carbon isotope composition of marine

phytoplankton. *Limnology and Oceanography*, 46(4), 996–998. https://doi.org/10.4319/lo.2001.46.4.0996

Eide, M., Olsen, A., Ninnemann, U. S., & Eldevik, T. (2017). A global estimate of the full oceanic $^{13}$C Suess effect since the preindustrial. *Global Biogeochemical Cycles*, 31(3), 492–514. https://doi.org/10.1002/2016GB005472

Elliott Smith, E. A., Tinker, M. T., Whistler, E. L., Kennett, D. J., Vellanoweth, R. L., Gifford-Gonzalez, D., Hylkema, M. G., & Newsome, S. D. (2020). Reductions in the dietary niche of southern sea otters (*Enhydra lutris nereis*) from the Holocene to the Anthropocene. *Ecology and Evolution*, 10(7), 3318–3329. https://doi.org/10.1002/ece3.6114

Espinasse, B., Pakhomov, E. A., Hunt, B. P. V., & Bury, S. J. (2019). Latitudinal gradient consistency in carbon and nitrogen stable isotopes of particulate organic matter in the Southern Ocean. *Marine Ecology Progress Series*, 631, 19–30. https://doi.org/10.3354/meps13137

Farmer, R. G., & Leonard, M. L. (2011). Long-term feeding ecology of Great Black-backed Gulls (*Larus marinus*) in the northwest Atlantic: 110 years of feather isotope data. *Canadian Journal of Zoology*, 89(2), 123–133. https://doi.org/10.1139/Z10-102

Giese, B. S., & Ray, S. (2011). El Niño variability in simple ocean data assimilation (SODA), 1871–2008. *Journal of Geophysical Research: Oceans*, 116(2), 1–17. https://doi.org/10.1029/2010JC006695

Gruber, N., Keeling, C. D., Bacastow, R. B., Guenther, P. R., Lueker, T. J., Wahlen, M., Meijer, H. A. J., Mook, W. G., & Stocker, T. F. (1999). Spatiotemporal patterns of carbon-13 in the global surface oceans and the oceanic Suess effect. *Global Biogeochemical Cycles*, 13(2), 307–335. https://doi.org/10.1029/1999GB900019

Guiry, E., Royle, T. C. A., Matson, R. G., Ward, H., Weir, T., Waber, N., Brown, T. J., Hunt, B. P. V., Price, M. H. H., Finney, B. P., Kaeriyama, M., Qin, Y., Yang, D. Y., & Szpak, P. (2020). Differentiating salmonid migratory ecotypes through stable isotope analysis of collagen: Archaeological and ecological applications. *PLoS ONE*, 15(4), 1–25. https://doi.org/10.1371/journal.pone.0232180

Halffman, C. M., Potter, B. A., McKinney, H. J., Finney, B. P., Rodrigues, A. T., Yang, D. Y., & Kemp, B. M. (2015). Early human use of anadromous salmon in North America at 11,500 y ago. *Proceedings of the National Academy of Sciences of the United States of America*, 112(40), 12344–12348. https://doi.org/10.1073/pnas.1509747112

Harris, A. J. T., Feuerborn, T. R., Sinding, M.-H., Nottingham, J., Knudsen, R., Rey-Iglesia, A., Schmidt, A. L., Appelt, M., Grønnow, B., Alexander, M., Eriksson, G., Dalén, L., Hansen, A. J., & Lidén, K. (2020). Archives of human-dog relationships: Genetic and stable isotope analysis of Arctic fur clothing. *Journal of Anthropological Archaeology*, 59, 101200. https://doi.org/10.1016/j.jaa.2020.101200

Hilton, G. M., Thompson, D. R., Sagar, P. M., Cuthbert, R. J., Cherel, Y., & Bury, S. J. (2006). A stable isotopic investigation into the causes of decline in a sub-Antarctic predator, the rockhopper penguin. *Global Change Biology*, 12(4), 611–625. https://doi.org/10.1111/j.1365-2486.2006.01130.x

Huang, B., Thorne, P. W., Banzon, V. F., Boyer, T., Chepurin, G., Lawrimore, J. H., Zhang, H.-M. (2017). NOAA extended reconstructed sea surface temperature (ERSST), version 5. https://doi.org/10.7289/V5T72FNM

Keeling, C. D. (1979). The Suess effect: $^{13}$Carbon-$^{14}$Carbon interrelations. *Environment International*, 2(4–6), 229–300. https://doi.org/10.1016/0160-4120(79)90005-9

Keeling, C. D., Piper, S. C., Bacastow, R. B., Wahlen, M., Whorf, T. P., Heimann, M., & Meijer, H. A. (2005). Atmospheric $CO_2$ and $^{13}CO_2$ exchange with the terrestrial biosphere and oceans from 1978 to 2000: Observations and carbon cycle implications. In I. T. Baldwin, M. M. Caldwell, G. Heldmaier, R. B. Jackson, O. L. Lange, H. A. Mooney, E.-D. Schulze, U. Sommer, J. R. Ehleringer, M. Denise Dearing, & T. E. Cerling (Eds.), *A history of atmospheric $CO_2$ and its effects on plants, animals, and ecosystems* (pp. 83–113). Springer.

Keeling, R. F., Graven, H. D., Welp, L. R., Resplandy, L., Bi, J., Piper, S. C., Sun, Y., Bollenbacher, A., & Meijer, H. A. J. (2017). Atmospheric evidence for a global secular increase in carbon isotopic discrimination of land photosynthesis. *Proceedings of the National Academy of Sciences of the United States of America*, 114(39), 10361–10366. https://doi.org/10.1073/pnas.1619240114

Kochi, S., Pérez, S. A., Tessone, A., Ugan, A., Tafuri, M. A., Nye, J., Zangrando, A. F. (2018). $\delta^{13}$C and $\delta^{15}$N variations in terrestrial and marine foodwebs of Beagle Channel in the Holocene. Implications for human paleodietary reconstructions. *Journal of Archaeological Science: Reports*, 18(September 2017), 696–707. https://doi.org/10.1016/j.jasrep.2017.11.036

Laney, S. R., & Sosik, H. M. (2014). Phytoplankton assemblage structure in and around a massive under-ice bloom in the Chukchi Sea. *Deep-Sea Research Part II: Topical Studies in Oceanography*, 105, 30–41. https://doi.org/10.1016/j.dsr2.2014.03.012

Laws, E. A., Popp, B. N., Cassas, N., & Tanimoto, J. (2002). 13C discrimination patterns in oceanic phytoplankton: Likely influence of $CO_2$ concentrating mechanisms, and implications for palaeoreconstructions. *Functional Plant Biology*, 29(2–3), 323–333. https://doi.org/10.1071/Pp01183

MacFarling Meure, C., Etheridge, D., Trudinger, C., Steele, P., Langenfelds, R., Van Ommen, T., Smith, A., & Elkins, J. (2006). Law Dome $CO_2$, $CH_4$ and $N_2O$ ice core records extended to 2000 years BP. *Geophysical Research Letters*, 33(14), 2000–2003. https://doi.org/10.1029/2006GL026152

Marañón, E. (2015). Cell Size as a key determinant of phytoplankton metabolism and community structure. *Annual Review of Marine Science*, 7, 241–264. https://doi.org/10.1146/annurev-marine-010814-015955

Matthews, C. J. D., & Ferguson, S. H. (2014). Spatial segregation and similar trophic-level diet among eastern Canadian Arctic/north-west Atlantic killer whales inferred from bulk and compound specific isotopic analysis. *Journal of the Marine Biological Association of the United Kingdom*, 94(6), 1343–1355. https://doi.org/10.1017/S0025315413001379

Mendelssohn, R. (2020). *Rerddapxtracto: Extracts environmental data from ERD's ERDDAP web service*. R package version 0.4.8. Retrieved from https://github.com/rmendels/rerddapXtracto

Menden-Deuer, S., & Lessard, E. J. (2000). Carbon to volume relationships for dinoflagellates, diatoms, and other protist plankton. *Limnology and Oceanography*, 45(3), 569–579. https://doi.org/10.4319/lo.2000.45.3.0569

Misarti, N., Finney, B., Maschner, H., & Wooller, M. J. (2009). Changes in northeast Pacific marine ecosystems over the last 4500 years: Evidence from stable isotope analysis of bone collagen from archeological middens. *The Holocene*, 19, 1139–1151. https://doi.org/10.1177/0959683609345075

Newsome, S. D., Phillips, D. L., Culleton, B. J., Guilderson, T. P., & Koch, P. L. (2004). Dietary reconstruction of an early to middle Holocene human population from the central California coast: Insights from advanced stable isotope mixing models. *Journal of Archaeological Science*, 31(8), 1101–1115. https://doi.org/10.1016/j.jas.2004.02.001

Polovina, J. J., & Woodworth, P. A. (2012). Declines in phytoplankton cell size in the subtropical oceans estimated from satellite remotely-sensed temperature and chlorophyll, 1998–2007. *Deep-Sea Research Part II: Topical Studies in Oceanography*, 77–80, 82–88. https://doi.org/10.1016/j.dsr2.2012.04.006

Quay, P., Sonnerup, R., Stutsman, J., Maurer, J., Körtzinger, A., Padin, X. A., & Robinson, C. (2007). Anthropogenic $CO_2$ accumulation rates in the North Atlantic Ocean from changes in the $^{13}C/^{12}C$ of dissolved inorganic carbon. *Global Biogeochemical Cycles*, 21(1), 1–15. https://doi.org/10.1029/2006GB002761

Quay, P., Sonnerup, R., Westby, T., Stutsman, J., & McNichol, A. (2003). Changes in the $^{13}C/^{12}C$ of dissolved inorganic carbon in the ocean as

a tracer of anthropogenic $CO_2$ uptake. *Global Biogeochemical Cycles*, *17*(1), 4-1–4-20. https://doi.org/10.1029/2001gb001817

Ramos, R., Reyes-González, J. M., Morera-Pujol, V., Zajková, Z., Militão, T., & González-Solís, J. (2020). Disentangling environmental from individual factors in isotopic ecology: A 17-year longitudinal study in a long-lived seabird exploiting the Canary Current. *Ecological Indicators*, *111*(December 2019), 105963. https://doi.org/10.1016/j.ecolind.2019.105963

Rau, G. H., Riebesell, U., & Wolf-Gladrow, D. (1996). A model of photosynthetic $^{13}$C fractionation by marine phytoplankton based on diffusive molecular $CO_2$ uptake. *Marine Ecology Progress Series*, *133*(1–3), 275–285. https://doi.org/10.3354/meps133275

Rossman, S., Barros, N. B., Ostrom, P. H., Stricker, C. A., Hohn, A. A., Gandhi, H., & Wells, R. S. (2013). Retrospective analysis of bottlenose dolphin foraging: A legacy of anthropogenic ecosystem disturbance. *Marine Mammal Science*, *29*(4), 705–718. https://doi.org/10.1111/j.1748-7692.2012.00618.x

Ruddiman, W. F. (2013). The anthropocene. *Annual Review of Earth and Planetary Sciences*, *41*, 45–68. https://doi.org/10.1146/annurev-earth-050212-123944

Schuster, U., Watson, A. J., Bates, N. R., Corbiere, A., Gonzalez-Davila, M., Metzl, N., Pierrot, D., & Santana-Casiano, M. (2009). Trends in North Atlantic sea-surface $fCO_2$ from 1990 to 2006. *Deep-Sea Research Part II: Topical Studies in Oceanography*, *56*(8–10), 620–629. https://doi.org/10.1016/j.dsr2.2008.12.011

Sea Surface Salinity-Near Real Time-MIRAS SMOS. (2020). Retrieved from https://coastwatch.noaa.gov/cw/satellite-data-products/sea-surface-salinity/miras-smos.html

Sherman, E., Moore, J. K., Primeau, F., & Tanouye, D. (2016). Temperature influence on phytoplankton community growth rates. *Global Biogeochemical Cycles*, *30*, 550–559. https://doi.org/10.1002/2015GB005272

Soto, D. X., Trueman, C. N., Samways, K. M., Dadswell, M. J., & Cunjak, R. A. (2018). Ocean warming cannot explain synchronous declines in North American Atlantic salmon populations. *Marine Ecology Progress Series*, *601*, 203–213. https://doi.org/10.3354/meps12674

Sun, J., Bustnes, J. O., Helander, B., Bårdsen, B.-J., Boertmann, D., Dietz, R., Jaspers, V. L. B., Labansen, A. L., Lepoint, G., Schulz, R., Søndergaard, J., Sonne, C., Thorup, K., Tøttrup, A. P., Zubrod, J. P., Eens, M., & Eulaers, I. (2019). Temporal trends of mercury differ across three northern white-tailed eagle (*Haliaeetus albicilla*) subpopulations. *Science of the Total Environment*, *687*, 77–86. https://doi.org/10.1016/j.scitotenv.2019.06.027

Vales, D. G., Cardona, L., Loizaga, R., García, N. A., & Crespo, E. A. (2020). Long-term stability in the trophic ecology of a pelagic forager LIving in a changing marine ecosystem. *Frontiers in Marine Science*, *7*(February), 1–10. https://doi.org/10.3389/fmars.2020.00087

Verburg, P. (2007). The need to correct for the Suess effect in the application of $\delta^{13}$C in sediment of autotrophic Lake Tanganyika, as a productivity proxy in the Anthropocene. *Journal of Paleolimnology*, *37*(4), 591–602. https://doi.org/10.1007/s10933-006-9056-z

Vokhshoori, N. L., McCarthy, M. D., Collins, P. W., Etnier, M. A., Rick, T., Eda, M., Beck, J., & Newsome, S. D. (2019). Broader foraging range of ancient short-tailed albatross populations into California coastal waters based on bulk tissue and amino acid isotope analysis. *Marine Ecology Progress Series*, *610*, 1–13. https://doi.org/10.3354/meps12839

Wang, H., Hu, X., & Sterba-Boatwright, B. (2016). A new statistical approach for interpreting oceanic $fCO_2$ data. *Marine Chemistry*, *183*, 41–49. https://doi.org/10.1016/j.marchem.2016.05.007

Watanabe, Y. W., Chiba, T., & Tanaka, T. (2011). Recent change in the oceanic uptake rate of anthropogenic carbon in the North Pacific subpolar region determined by using a carbon-13 time series. *Journal of Geophysical Research: Oceans*, *116*(2), 1–10. https://doi.org/10.1029/2010JC006199

Weiss, R. F. (1974). Carbon dioxide in water and seawater: The solubility of a non-ideal gas. *Marine Chemistry*, *2*, 203–215. https://doi.org/10.1016/0304-4203(74)90015-2

Weiss, R. F., & Price, B. A. (1980). Nitrous oxide solubility in water and seawater. *Marine Chemistry*, *8*, 347–359. https://doi.org/10.1017/CBO9781107415324.004

Young, J. N., Bruggeman, J., Rickaby, R. E. M., Erez, J., & Conte, M. (2013). Evidence for changes in carbon isotopic fractionation by phytoplankton between 1960 and 2010. *Global Biogeochemical Cycles*, *27*(2), 505–515. https://doi.org/10.1002/gbc.20045

Zangrando, A. F., Riccialdelli, L., Kochi, S., Nye, J. W., & Tessone, A. (2016). Stable isotope evidence supports pelagic fishing by hunter-gatherers in southern South America during the Late Holocene. *Journal of Archaeological Science: Reports*, *8*, 486–491. https://doi.org/10.1016/j.jasrep.2016.05.015

## SUPPORTING INFORMATION

Additional supporting information may be found online in the Supporting Information section.